

## Optimization of EDM process for multiple performance characteristics using Taguchi method and Grey relational analysis<sup>†</sup>

Jong Hyuk Jung and Won Tae Kwon<sup>\*</sup>

*Department of Mechanical and Information Engineering, University of Seoul, Seoul, 130-743, Korea*

(Manuscript Received September 24, 2009; Revised November 2, 2009; Accepted November 30, 2009)

### Abstract

Electrical discharge machining (EDM) is one of the most extensively used non-conventional material removal processes. The Taguchi method has been utilized to determine the optimal EDM conditions in several industrial fields. The method, however, was designed to optimize only a single performance characteristic. To remove that limitation, the Grey relational analysis theory has been used to resolve the complicated interrelationships among the multiple performance characteristics. In the present study, we attempted to find the optimal machining conditions under which the micro-hole can be formed to a minimum diameter and a maximum aspect ratio. The Taguchi method was used to determine the relations between machining parameters and process characteristics. It was found that electrode wear and the entrance and exit clearances had a significant effect on the diameter of the micro-hole when the diameter of the electrode was identical. Grey relational analysis was used to determine the optimal machining parameters, among which the input voltage and the capacitance were found to be the most significant. The obtained optimal machining conditions were an input voltage of 60V, a capacitance of 680pF, a resistance of 500Ω, the feed rate of 1.5μm/s and a spindle speed of 1500rpm. Under these conditions, a micro-hole of 40μm average diameter and 10 aspect ratio could be machined.

*Keywords:* Electrical discharge machining (EDM); Taguchi method; Grey relational analysis

### 1. Introduction

Electrical discharge machining (EDM) is one of the most extensively used non-conventional material removal processes. Its unique feature, that is, the use of thermal energy to machine electrically conductive parts regardless of hardness has been its distinctive advantage in the manufacture of moulds, dies, automotive, as well as aerospace and surgical components. The growing popularity of micro-EDM can be attributed to advantages including low set-up cost, high-aspect-ratio parts, enhanced precision, and significant design freedom [1]. Another characteristic of EDM is the lack of direct contact between the electrode and the workpiece, thus eliminating mechanical stress, chatter and vibration during machining [2]. Masuzawa fabricated micro pins, micro nozzles and micro pipes using EDM [3-6] and Allen used micro-EDM technology to manufacture ink jet nozzles [7]. Liu presented a process using micro-EDM combined with high-frequency dither grinding (HFDG) to improve the surface roughness of micro-holes [8]. Jahan investigated the influence of major operating

parameters on the performance of micro-EDM with an electrode of WC in producing quality micro-holes in both transistor- and RC-type generators [9]. Research into micro holes with aspect ratios above 10 [9-11] also has been conducted over the years. However, the average diameter of the machined micro holes is above 80μm, and therefore to obtain specimens of smaller diameter and higher aspect ratio, the machining parameters must be optimized. The Taguchi method has been widely employed in several industrial fields and relevant research work. Liao et al. used the Taguchi method to determine the optimal parameter settings in Wire-EDM [12]. Lin et al. adopted the method to obtain the optimal machining parameters of a hybrid process of EDM incorporating ball-burnish machining [13]. The original Taguchi method was designed to optimize only a single performance characteristic. The Grey relational analysis theory posited by Deng [14] has been proved to effectively resolve the complicated interrelationships among multiple performance characteristics of the EDM process [15-17]. Specifically, Deng, using EDM, optimized the material removal rate (MRR), the surface roughness (SR) and the tool wear ratio (TWR) [15], and later, for the machining of Al-10%SiCp by EDM, the MRR, TWR, SR, taper (T) and radial overcut (ROC) were likewise optimized [16].

<sup>†</sup> This paper was recommended for publication in revised form by Associate Editor Dae-Eun Kim

<sup>\*</sup> Corresponding author. Tel.: +82 2 2210 2403, Fax.: +82 2 2210 5575

E-mail address: kwon@uos.ac.kr

© KSME & Springer 2010

The goal of the present study was to determine the optimal machining parameters for formation of micro-holes of minimum diameter and maximum aspect ratio under given machining conditions. The Taguchi method was employed to elucidate the effect of the machining parameters on the characteristics of the EDM process. Additionally, Grey relational analysis was used to find the optimal machining parameters satisfying the multiple characteristics of the EDM process.

## 2. Machining of micro-hole using EDM

### 2.1 Experimental set-up

In a home-made EDM machine used in this study, three linear DC motor (Dover, Trilogy LM-210) and a controller (Computer, CM233AX) were installed to control displacement in each of the X, Y and Z directions, respectively. An encoder (Heidenhain LIP401A) with the resolution of 0.1m/count was mounted on each axis to relay high-precision displacement information to the controller. A smart motor (Antimatics Inc. 2315D DC brushless type) along with a static pneumatic bearing were installed in the spindle system in order to achieve 0.05 $\mu$ m rotation precision in the radial direction and up to 3000rpm rotational spindle speed. Removal of debris generated during the machining process being indispensable to maintaining smooth processing during EDM machining, the electrode rotation technique was selected over the ultrasonic vibration and internal/external flushing debris-removal-technology alternatives. We chose an RC circuit to provide discharge energy, owing to the attendant ease of control of discharge energy using voltage and capacitance [9]. Positive-polarity machining by means of a negative electrical source connected to the electrode and a positive electrical source connected to the work material, was utilized. This type of machining allowed us a higher machining rate along with lesser electrode wear [11]. The electrode was produced by WEDM (wire-EDM) machining. An induction motor (SPG cop. S6106GB-V12) was installed to transfer the brass wire at a constant speed of 40mm/min.. Also a constant tension of 3.5N was maintained during electrode machining using a hysteresis clutch break PHT-1 (Ogura clutch cop.) to minimize the deviation of the wire from the trajectory.

### 2.2 Machining of electrode

The electrode, as already stated, was produced by WEDM machining [3]. Reduction of the electrode diameter due to wire wear was minimized by means of the constant speed of wire transfer and consistent wire tension just noted. The WC electrode, of 50mm length and 300 $\mu$ m diameter was machined into a smaller diameter electrode using WEDM processing. A relatively large discharge energy (>18 $\mu$ J) was used in rough formation of the electrode, followed by the finishing processing utilizing a much smaller energy (<4 $\mu$ J). The electrode wear in the axial direction with kerosene as the dielectric fluid was twice that with de-ionized water as dielectric fluid [10].

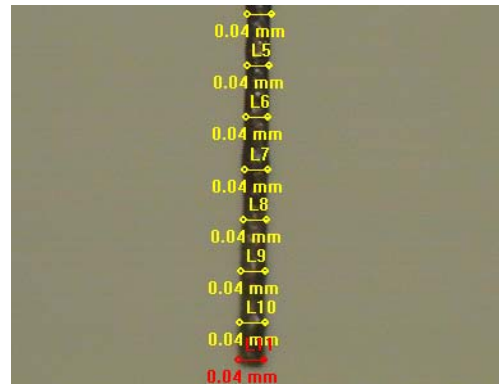


Fig. 1. Measurement of electrode diameter using image processing technology ( $\sigma = 2.53\mu$ m).

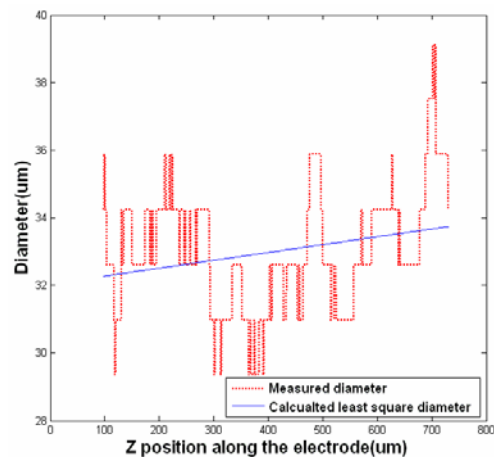


Fig. 2. Measured and calculated diameter along electrode.

Taking this phenomenon and the depth of the hole (400 $\mu$ m) into consideration, the length of the electrode was determined to be 1300 $\mu$ m. Whereas the manufacturing tolerance of the electrode is not a significant issue in general EDM processing, in micro-EDM processing it certainly is. An automatic image-processing method was developed to provide the necessarily precise electrode diameter measurement. In this method, first, the image of the electrode is captured by microscope, after which image-processing technology is utilized to detect the electrode edge. With the least square method, two straight lines off the edge in the axial direction are drawn, and then the center line is obtained by taking the average of the two straight lines. By means of a line drawn perpendicular to the center line, the diameter of the electrode can be determined. Fig. 1 shows the measured diameter at several points of the electrode along the rotational axis, and Fig. 2 shows both the measured diameter and the calculated least square diameter based on same. We then proceeded to find the optimal machining conditions under which the electrode, using the Taguchi method, can be manufactured as quickly as possible. Several tens of experiments showed that the accuracy of the electrode is influenced more by the experience of the worker than by the processing parameters.

Table 1. Machining condition for EDM processing.

Electrode	Material	WC
	Diameter ( $\mu\text{m}$ )	30 ~ 36
Work material	Material	SS 304
	Thickness ( $\mu\text{m}$ )	400
Dielectric fluid	Kerosene	
Experimental condition	Voltage (V)	60, 110
	Capacitance (pF)	680, 1300, 2000
	Resistance ( $\Omega$ )	500, 1500, 3000
	Feed rate ( $\mu\text{m/s}$ )	1, 1.5, 2
	RPM	1500, 2200, 2900

Table 2. Experimenter's log and experiment results.

No	Voltage (V)	Capacitance (pF)	Resistance ( $\Omega$ )	Feed rate ( $\mu\text{m/s}$ )	Tool rotational speed (RPM)	Time (s)	Electrode Wear ( $\mu\text{m}$ )	Entrance clearance ( $\mu\text{m}$ )	Exit clearance ( $\mu\text{m}$ )	No. of Shorts
1	60	680	500	1	1500	3480	431	6.57	1.26	321
2	60	680	1500	1.5	2200	1800	468	5.35	1.65	53
3	60	680	3000	2	2900	1440	457	7.105	3.415	19
4	60	1300	500	1	2200	1860	307	7.29	3.09	64
5	60	1300	1500	1.5	2900	1500	378	6.625	2.575	22
6	60	1300	3000	2	1500	1800	546	7.99	1.98	70
7	60	2000	500	1.5	1500	2640	362	6.335	0.685	275
8	60	2000	1500	2	2200	2040	522	6.78	0.63	130
9	60	2000	3000	1	2900	1920	474	6.335	1.145	21
10	110	680	500	2	1500	1500	479	11.465	3.155	17
11	110	680	1500	1	1500	2100	542	10.285	0.495	30
12	110	680	3000	1.5	2200	1560	445	10.105	3.055	20
13	110	1300	500	1.5	2900	1980	605	9.815	1.045	46
14	110	1300	1500	2	1500	1620	554	11.8	1.68	27
15	110	1300	3000	1	2200	2040	515	12.085	0.495	20
16	110	2000	500	2	2200	2220	767	11.205	1.145	81
17	110	2000	1500	1	2900	2220	639	11.08	5.4	9
18	110	2000	3000	1.5	1500	1800	518	12.58	3.51	42

It has also been revealed that the most important factor in machining the smallest hole with the maximum aspect ratio is the diameter of the electrode. It is generally accepted that minimal-diameter micro-hole requires an even smaller-diameter electrode. However, there is a limitation of the diameter on how small the diameter of an electrode can be. According to our preliminary experiments, an electrode with the diameter below 25–30 $\mu\text{m}$  could not stand the harsh environment of EDM processing, and accordingly would break. Breakage may be attributed specially to the collision of an electrode with the work material. Hence, we manufactured an

electrode of 30–36 $\mu\text{m}$  diameter for use in our experiments.

### 2.3 Machining of micro hole

In the course of the EDM process, discharging occurs when the electrode and the work material are closed enough to induce a spark. If the electrode touches the work material during machining, meaning that sparks have not been induced, the z axis of the machine retreats backward to make a gap. The voltage difference between the electrode and the work material is then measured to determine whether the electrode and the work material have been short-circuited or not. After the machining is completed, the wear length of the electrode is measured by touching it to the un-machined surface of the work material and calculating the difference in the z axis before and after machining. When the diameter of the micro-hole to be machined is over 70–80 $\mu\text{m}$ , the machining time and electrode wear are shorter when the dielectric fluid is water. However, for a smaller micro-hole, kerosene is more effective [10], which is confirmed in our experiment.

## 3. Experiments and results

### 3.1 Experimental condition

The purpose of the experiments was to form a micro hole of maximum aspect ratio and minimum diameter. From the result of our preliminary experiments, we settled on the use of a 400 $\mu\text{m}$  thickness SS304 work material to machine a maximum aspect ratio micro-hole. WC of 30–36 $\mu\text{m}$  diameter and 1300 $\mu\text{m}$  length was manufactured for use as an electrode. To determine the machining conditions suitable for a hole of maximum aspect ratio and minimum diameter machined with a home-made electrode, the Taguchi method was used. The selected machining parameters, listed in Table 1, were voltage, capacitance, resistance, feed rate and spindle speed. An  $L_{18}$  ( $2^1 \times 3^7$ ) orthogonal array was selected to determine the 18 trial conditions and their results, tabulated in Table 2. Two levels of voltage were selected along with three levels of capacitance, resistance, feed rate and spindle speed.

### 3.2 Result of experiment

The results of the experiment are illustrated in Fig. 3, and the quantitative results for electrode wear, entrance clearance, exit clearance, machining time and number of shorts are listed in Table 3. Entrance clearance indicated the difference between the radius of the electrode and the machined micro-hole at the micro-hole entrance. Exit clearance, correspondingly, is the difference between the radius of the electrode and the machined hole at the micro-hole exit. Accordingly, we wanted these two clearances to be as tight as possible so as to machine the smallest micro-hole. In the ideal case, this value would be 0, meaning that the diameters of the electrode and the micro hole are identical.

Table 3. Experimental results by Taguchi method.

		Electrode wear (μm)	Entrance clearance (μm)	Exit clearance (μm)	Machining time (s)	No. of Shorts
Voltage (V)	60	438	6.7	1.8	2053	108
	110	563	10.7	2.2	1893	32
Capacitance (pF)	680	470	8.5	2.2	1980	77
	1300	484	9.3	1.8	1800	42
	2000	547	9.1	2.1	2140	93
Resistance (Ω)	500	492	8.8	1.7	2280	134
	1500	517	8.7	2.1	1880	45
	3000	493	9.4	2.3	1760	32
Feedrate (μm/s)	1	485	8.9	2.0	2270	78
	1.5	463	8.5	2.1	1880	76
	2	554	9.4	2.0	1770	57
RPM	1500	492	9.3	1.6	2240	128
	2200	504	8.8	1.7	1920	61
	2900	505	8.7	2.8	1760	22

Table 4. Electrical characteristics according to variation of voltage, capacitance and resistance.

		Peak current (I)	Discharge power (W)	Discharge energy (μJ)
Voltage (V)	60	3.78	0.59	2.39
	110	5.77	1.98	8.03
Capacitance (pF)	680	3.50	1.28	2.67
	1300	4.83	1.28	5.10
	2000	5.99	1.29	7.85
Resistance (Ω)	500	4.77	2.55	5.21
	1500	4.77	0.87	5.21
	3000	4.77	0.43	5.21

3.2.1 Analysis of the results according to the input voltage variation

When the voltage increased from 60V to 110V, the electrode wear increased from 438μm to 563μm. For the sacrifice of electrode wear, the machining time was reduced from 2053sec. to 1893sec. Both the entrance and exit clearance increased at the same time. The number of shorts changed from 108 to 32. The discharge energy in each case increased from 2.39μJ to 8.03μJ, as indicated in Table 4. With the same input voltage increase (from 60V to 110V), the electrode wear, the entrance and exit clearances and the discharge energy all increased, while the machining time and number of shorts decreased. Those phenomena could be attributed to the increased input voltage that led to the increased discharge energy. The increased discharge energy resulted in a larger sparks, which removed the debris generated during the machining quite effectively. The higher discharge energy resulted in accelerated electrode wear and increased entrance and exit

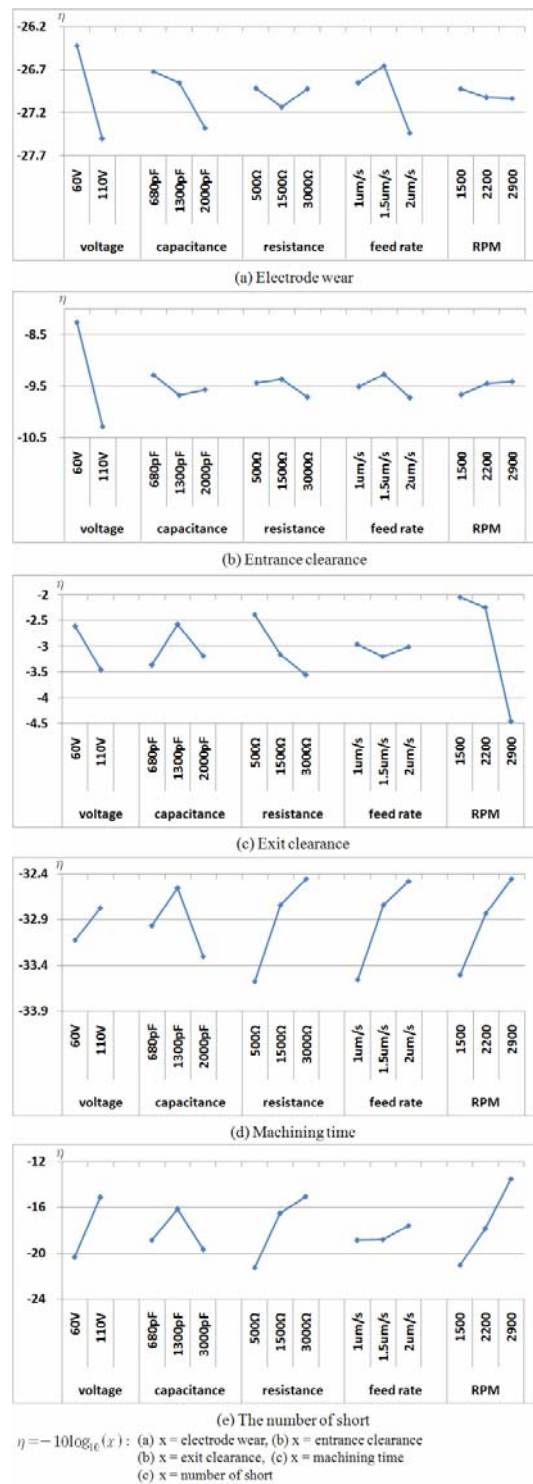


Fig. 3. Plots of factor effects.

clearances, while the successful removal of the debris effected decreases in the machining time and the number of shorts.

3.2.2 Analysis of the results according to the capacitance variation

As the capacitance increased from 680pF to 2000pF, the

electrode wear and the machining time rose from 470 $\mu\text{m}$  to 547 $\mu\text{m}$  and from 1980sec. to 2140sec., respectively. The entrance and exit clearances and the number of shorts remained almost the same. The increased electrode wear could be attributed to the increased discharge energy.

### 3.2.3 Analysis of the results according to the resistance variation

The machining parameters most influenced by the variation of the resistance were the machining time and the number of shorts. As the resistance increased from 500 $\Omega$  to 3000 $\Omega$ , the machining time and the number of shorts decreased from 2280sec. to 1760sec. and from 134 to 32, respectively. As can be seen in Table 4's results, as the resistance increased, so too did the discharge power decrease. This decrement of the discharge energy caused a reduction in the debris size, which led to a reduction in the number of shorts and in the machining time. The variation of the electrode wear in the axial direction as was that of the entrance and exit clearances, was negligible.

### 3.2.4 Analysis of the results according to feed rate variation

The feed rate variation greatly affected the electrode wear and the machining time. When the feed rate changed from 1 $\mu\text{m}/\text{sec.}$  to 1.5 $\mu\text{m}/\text{sec.}$ , the machining time was reduced from 2270sec. to 1880sec. and the electrode wear decreased from 485 $\mu\text{m}$  to 463 $\mu\text{m}$ . The 1.5 $\mu\text{m}/\text{sec.}$  feed rate showed a better result in both machining time and electrode wear. This meant that the interval between discharges was long enough to recharge the circuit when the feed rate was either 1 $\mu\text{m}/\text{sec.}$  or 1.5 $\mu\text{m}/\text{sec.}$  As a result, the increment of the feed rate did not change the discharge energy but only reduced the machining time. The electrode wear did not change significantly in this case. By contrast, as the feed rate increased from 1.5 $\mu\text{m}/\text{sec.}$  to 2 $\mu\text{m}/\text{sec.}$ , the electrode wear increased and the machining time decreased. An increment of the feed rate to 2 $\mu\text{m}/\text{sec.}$  resulted in their being insufficient time for recharge of the circuit. Because of the insufficient amount of energy resulting from the insufficient recharging time, there was an insufficient amount of discharge energy compared with the case for the feed rates of 1 $\mu\text{m}/\text{sec.}$  and 1.5 $\mu\text{m}/\text{sec.}$  Consequently, we needed to increase the number of discharges to finish the machining. And due to the enhanced number of discharges, the electrode wear also increased.

The discharge energy decrement and the feed rate increment had opposite effect on the machining time. When the discharge energy decreased, the machining time increased accordingly. But when the feed rate increased, the machining time decreased. In this experiment, the effect of the increased feed rate was larger than that of the decreased discharge energy. Resultantly, the machining time and the number of shorts decreased as the feed rate increased to 2.0 $\mu\text{m}/\text{sec.}$  and the discharge energy decreased. This meant that even though the discharge energy was reduced because of the increased feed rate, it was yet sufficient speed of the electrode to induce a spark between the electrode and the work material.

### 3.2.5 Analysis of results according to the spindle speed variation

It is known that the spindle speed has one of the most significant effects on the removal of debris generated in the EDM process [18]. In the present experimentation, as the spindle speed increased from 1500, via 2200, to 2900rpm, the number of shorts decreased from 128, via 61, to 22. The machining time also decreased from 2240, via 1920, to 1760sec.. As the spindle speed increased, the debris was removed more quickly, which led to a reduced number of shorts and a shorter machining time. The electrode wear and the entrance clearance remained almost identical. The exit clearance increased from 1.6 $\mu\text{m}$  to 2.8 $\mu\text{m}$ .

### 3.2.6 Relationship between electrical characteristics and electrical parameter

Eqs. (1), (2), (3) show the relationships between electrical characteristics and input voltage, capacitance and resistance, respectively [17]. The calculated results are given in Table 4.  $V_{\text{gap}}$  and  $L_2$  (inductance) are 26.5V and 0.2 $\mu\text{H}$ , respectively.

$$I_p \approx \frac{V - V_{\text{gap}}}{\sqrt{L_2/C}} \quad (1)$$

$$W = \frac{1}{2} CV^2 \frac{1}{-R_1 C \ln(1 - V_d/V) + \pi \sqrt{L_2 C}} \quad (2)$$

$$E_{\text{unit,RC}} = \frac{1}{2} CV^2 \quad (3)$$

## 3.3 Determination of the machining condition

In the previous section, it was shown that the electrode wear and entrance and exit clearances are directly related to the size of the micro-hole in 5 of machining process characteristics. The machining time and the number of shorts does not show a significant relation to the size of the micro-hole, which, rather, is related to productivity. As a result, the electrode wear along with the entrance and exit clearances were determined to be the parameters to optimize in order to minimize the hole size. We had to determine the machining parameters such the input voltage, capacitance, resistance, the feed rate and the spindle speed to optimize the electrode wear and entrance and exit clearance characteristics. It is a complicated procedure to determine 5 machining parameters for optimizing 3 characteristics. To overcome the difficulty, Grey relational analysis was employed [14].

### 3.3.1 Grey relational analysis

The original reference sequence and the sequence for comparison can be represented as  $x_0(k)$  and  $x_i(k)$ ,  $i=1, 2, \dots, m$ ;  $k=1, 2, \dots, n$  respectively. Here,  $m$  is the total number of experiments, while  $n$  is the total number of observation data. If the target value of the original sequence is 'the-larger-the-better', then the original sequence is normalized according to

$$x_i^*(k) = \frac{x_i^o(k) - \min x_i^o(k)}{\max x_i^o(k) - \min x_i^o(k)} \quad (4)$$

If it is 'the-smaller-the-better', then the original sequence is normalized as

$$x_i^*(k) = \frac{\max x_i^o(k) - x_i^o(k)}{\max x_i^o(k) - \min x_i^o(k)} \tag{5}$$

In the case where there is 'a specific value', the original sequence is normalized as

$$x_i^*(k) = 1 - \frac{|x_i^o(k) - OB|}{\max \{ \max x_i^o(k) - OB, OB - \min x_i^o(k) \}} \tag{6}$$

Here, OB is the target value.

**3.3.2 Grey relational coefficient and Grey relational grades**

The Grey relational coefficient is defined as follows [14]

$$\gamma(x_o^*(k), x_i^*(k)) = \frac{\Delta_{\min} + \zeta \Delta_{\max}}{\Delta_{oi}(k) + \zeta \Delta_{\max}} \tag{7}$$

$$0 < \gamma(x_o^*(k), x_i^*(k)) \leq 1$$

$\Delta_{oi}(k)$  is the deviation sequence of the reference sequence  $x_o^*(k)$  and the comparability sequence  $x_i^*(k)$ , that is:

$$\Delta_{oi}(k) = |x_o^*(k) - x_i^*(k)|$$

$$\Delta_{\max} = \max_{\forall j \in i} \max_{\forall k} |x_o^*(k) - x_j^*(k)| \tag{8}$$

$$\Delta_{\min} = \min_{\forall j \in i} \min_{\forall k} |x_o^*(k) - x_j^*(k)|$$

where  $\zeta$  is the distinguishing coefficient,  $\zeta \in [0,1]$ .

A Grey relational grade is a weighted sum of the Grey coefficient, and is defined as

$$\gamma(x_o^*, x_i^*) = \sum_{k=1}^n \beta_k \gamma(x_o^*(k), x_i^*(k)) \tag{9}$$

$$\sum_{k=1}^n \beta_k = 1$$

Here the Grey relational grade  $\gamma(x_o^*, x_i^*)$  represents the level of correlation between the reference and the comparability sequence. If a particular comparability sequence is more important to the reference sequence than the other comparability sequence, the Grey relational grade for that comparability sequence and the reference sequence will exceed that for the other Grey relational grades.

**3.3.3 Evaluated Grey relational coefficient and grade**

The experimental results for the electrode wear, the entrance clearance and the exit clearance are listed in Table 2. Since smaller values for those parameters were desirable, the data sequence had 'the-smaller-the-better' characteristic. Hence, Eq. (5) is employed for the data processing, the results of which are listed in Table 5. Eq. (7) was utilized to determine the Grey relational coefficient, and Eq. (9) the Grey rela-

Table 5. Experimental results after normalization process (Reference sequence for all parameters is 1).

	Electrode wear	Entrance clearance	Exit clearance
1	0.7304	0.8313	0.8440
2	0.6500	1.0000	0.7645
3	0.6739	0.7573	0.4047
4	1.0000	0.7317	0.4709
5	0.8457	0.8237	0.5759
6	0.4804	0.6349	0.6972
7	0.8804	0.8638	0.9613
8	0.5326	0.8022	0.9725
9	0.6370	0.8638	0.8675
10	0.6261	0.1542	0.4577
11	0.4891	0.3174	1.0000
12	0.7000	0.3423	0.4781
13	0.3522	0.3824	0.8879
14	0.4630	0.1079	0.7584
15	0.5478	0.0685	1.0000
16	0.0000	0.1902	0.8675
17	0.2783	0.2075	0.0000
18	0.5413	0.0000	0.3853

Table 6. Calculated Grey relational coefficient and grade.

	Grey relational coefficient			Grey relational grade
	Electrode wear	Entrance clearance	Exit clearance	
1	0.6497	0.7477	0.7622	0.7196
2	0.5882	1.0000	0.6798	0.7556
3	0.6053	0.6732	0.4565	0.5781
4	1.0000	0.6508	0.4859	0.7119
5	0.7641	0.7393	0.5411	0.6812
6	0.4904	0.5779	0.6229	0.5635
7	0.8070	0.7859	0.9281	0.8400
8	0.5169	0.7166	0.9478	0.7268
9	0.5793	0.7859	0.7905	0.7183
10	0.5721	0.3715	0.4797	0.4743
11	0.4946	0.4228	1.0000	0.6390
12	0.6250	0.4319	0.4893	0.5152
13	0.4356	0.4474	0.8168	0.5664
14	0.4822	0.3592	0.6742	0.5050
15	0.5251	0.3493	1.0000	0.6246
16	0.3333	0.3817	0.7905	0.5017
17	0.4093	0.3868	0.3333	0.3763
18	0.5215	0.3333	0.4486	0.4343

tional grade. The results are tabulated in Table 6. In this case, the reference sequences were set to 1, that is,  $x_i^*(k)=1$ , and the distinguishing coefficient  $\zeta$  was set to 0.5.

**3.3.4 ANOVA results for Grey grade**

Table 7 lists the results of the analysis of variance

Table 7. Results of analysis of variance (ANOVA).

Factor	Level 1	Level 2	Level 3	DOF	Sum of square	Mean square	F value	Contribution
Voltage	0.700	0.515		1	1.158	1.158	97.00	66.29
Capacitance	1.238	0.609	0.600	2	1.154	0.577	48.32	33.02
Resistance	0.636	0.614	0.573	2	0.006 <sup>+</sup>	0.003		
Feed rate	0.632	0.632	0.558	2	0.011 <sup>+</sup>	0.005		
Cutting speed	0.578	0.60	0.644	2	0.007 <sup>+</sup>	0.003		
Error				(6)	(0.024)	0.012		
Total				9	2.336	1.747		99.32

<sup>+</sup> Indicates the sum of squares added together to form the pooled error sum of squares shown in parentheses

(ANOVA) for the electrode wear, entrance clearance and exit clearance using the calculated values for the Grey relational coefficients and Grey relational grades of Table 6. The Table 7 figures show that the contributions of the voltage and capacitance were 66.29 and 33.02, respectively. These two were found to be the most significant controlling parameters, meaning that they controlled the electrode wear, entrance clearance and exit clearance simultaneously and very effectively.

**3.3.5 Determination of process parameters**

According to the ANOVA analysis of the Grey relational grades discussed in 3.3.4, the most significant factors were the voltage and capacitance, the values for which were 60V and 680pF, respectively. Since the remaining parameters were insignificant, their values were taken from Table 3: resistance 500Ω, feed rate 1.5μm/s, spindle speed 1500RPM. To prove the effectiveness of the selected optimal machining conditions, a confirmation experiment was executed using an electrode with a diameter of 30.6μm. It was shown that the machined micro-hole had an average diameter of 40μm and an aspect ratio of 10. The entrance and exit diameter were 45μm and 35μm respectively, as shown in Fig. 4. The electrode wear was 273μm, while the entrance and exit clearances were 7.49μm and 2.06μm, respectively. Compared with the Table 3 results, the electrode wear was the smallest, while the entrance clearance was close to the smallest. The exit clearance did not show any significant improvement. This was natural, considering that the average and standard deviations of exit clearance are 2.03μm and 0.31μm, respectively. The number of shorts in the z direction of the electrode are indicated in Fig. 5. As can be seen, the number linearly increased as the depth of the hole increased. This speaks to the consistency of the EDM process in forming the smallest microhole under the given conditions.

**4. Conclusions**

In this study, we attempted to find the optimal machining

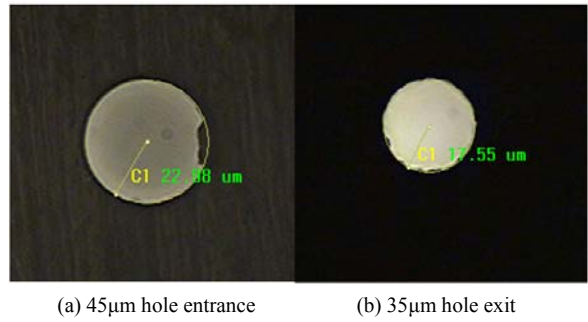


Fig. 4. Micro-hole machined under selected optimal condition (kerosene, 60V, 680pF, 500Ω, 1.5μm/s, 1500RPM).

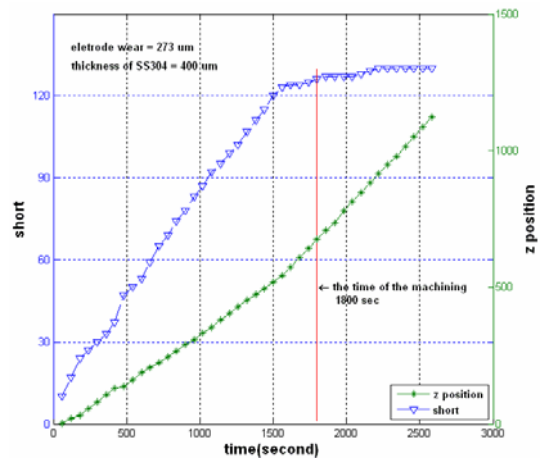


Fig. 5. Number of shorts and position of electrode in z direction for length of time.

conditions for drilling of a micro-hole of minimum diameter and maximum aspect ratio. The Taguchi method was employed to determine the relations between the machining parameters and the process characteristics. The machining parameters affecting the hole diameter were revealed by executing 18 experiments. It was found that the electrode wear and the entrance and exit clearances have a significant effect on the diameter of the micro-hole when the diameter of the electrode is identical. To determine the machining parameters affecting the electrode wear and the entrance and exit clearances, Grey relational analysis was used. The input voltage and the capacitance were found to be the most significant controlling parameters. The obtained optimal machining condition were an input voltage of 60V, a capacitance of 680pF, a resistance of 500Ω, a feed rate of 1.5μm/s and a spindle speed of 1500rpm. Under these conditions, a micro-hole of 40μm average diameter and an aspect ratio of 10 could be machined.

**Acknowledgement**

This work was supported by Nuclear Research & Development Program of the Korea Science and Engineering Foundation (KOSEF) grant funded by the Korean government (MEST) (grant code: M2009-0078442).

## References

- [1] H. S. Lim, Y. S. Wong, M. Rahman and M. K. Edwin Lee, A study on the machining of high-aspect ratio micro-structure using micro-EDM, *J. Mater. Process. Technol.*, 140 (2003) 318-325.
- [2] K. H. Ho and S. T. Newman, State of the art electrical discharge machining (EDM), *Int. J. Mach. Tools Manuf.*, 43 (2003) 1287-1300.
- [3] T. Masuzawa, M. Fujino and K. Kobayashi, Wire Electro-discharge grinding for Micro-machining, *Ann CIRP.*, 34 (1) (1985) 431-434.
- [4] T. Masuzawa, C. L. Kuo and M. Fujino, A combined Electrical Machining Process for Micro Nozzle Fabrication, *Ann CIRP.*, 43 (1) (1994) 189-192.
- [5] Z. Y. Yu, T. Masuzawa and M. Fujino, Micro-EDM for Three-dimensional Cavities-development of Uniform wear method, *Ann CIRP.*, 47 (1) (1998) 169-172.
- [6] C. L. Kuo and T. Masuzawa, a Micro-pipe fabrication process, *Proc. IEEE MEMS '91*, 80-85.
- [7] D. M. Allen and A. Lecheheb, Micro Electro-discharge Machining of Ink Jet Nozzle: Optimum Selection of Material and Machining Parameter, *J. Mat. Proc. Tech.*, 58 (1996) 53-63.
- [8] H. S. Liu, B. H. Yan, C. L. Chen and F. Y. Huang, Application of micro-EDM combined with high-frequency dither grinding to micro-hole machining, *Int. J. Mach. Tools Manuf.*, 46 (2006) 80-87.
- [9] M. P. Jahan, Y. S. Wong and M. Rahman, A study on the quality micro-hole machining of tungsten carbide micro-EDM process using transistor and RC-type pulse generator, *Int. Mater. Proc. Tech.*, 209 (2009) 1706-1716.
- [10] D. W. Seo, M. S. Park, S. M. Yi and C. N. Chu, Machining Characteristics of Micro-EDMed holes According to Dielectric Fluid, Capacitance and Ultrasonic Vibration, *J. Korean Soc. Precision Eng.*, 24 (2007) 42-29.
- [11] G. M. Kim, B. H. Kim and C. N. Chu, Machining Rate and Electrode Wear Characteristics in Micro-EDM of Micro-hole, *J. Korean Soc. Precision Eng.*, 16 (1999) 94-100.
- [12] Y. S. Liao, J. T. Huang and H. C. Su, A study on the machining-parameters optimization of wire electrical discharge machining, *J. Mater. Process. Technol.*, 71 (1997) 487-493.
- [13] Y. C. Lin, B. H. Yan and F. Y. Huang, Surface modification of Al-Zn-Mg aluminum alloy using combined processes of EDM with USM, *J. Mater. Process. Technol.*, 115 (2001) 359-366.
- [14] J. Deng, Introduction to Grey system, *J. of Grey System*, 1 (1) (1989) 1-24.
- [15] J. L. Lin and C. L. Lin, The use of the orthogonal array with Grey relational analysis to optimize the electrical discharge machining process with multiple performance characteristics, *Int. J. Mach. Tools Manuf.*, 42 (2002) 237-244.
- [16] P. N. Singh, K. Raghukandan and B. C. Pai, Optimization by Grey relational analysis of EDM parameters on machining Al-10% SiCp composites, *J. Mater. Process. Technol.*, 155-156 (2004) 1658-1661.
- [17] P. J. Cho, Characteristics of RC circuit with Transistor in Micro-EDM, Seoul National University (2003) Ph. D. Dissertation.
- [18] J. S. Soni and G. Chakraverti, Machining characteristics of titanium with rotary electro-discharge machining, *Wear*, 171 (1994) 51-58.



**Jong Hyuk Jung** received his B.S. and M.S in Mechanical Information Engineering from University of Seoul. He is currently an associate director in Industrial Application R&D Institute in DAEWOO SHIPBUILDING & MARINE ENGINEERING. He is involved in developing robots for productivity

improvement and systems for welding and painting automation.



**Won Tae Kwon** received his B.S., M.S. degree from Seoul National University, and Ph.D. degree from Northwestern University in 1982, 1984 and 1992, respectively. Prof. Kwon is currently a Professor of the Department of Mechanical and Information Engineering of University of Seoul, Korea. His research

fields include micro machining and machining process optimization.